Politecnico di Milano
MSc Space Engineering

Attitude Control of a 16U CubeSat. Detumbling and tracking.

Professor:
Biggs,James Douglas

Author:
de Miguel ,Alejandro
{918897}

Contents

1 Mission and spacecraft characteristics

In this report the attitude control of a 16 units cubesat will be shown. Firstly, the mission constraints and spacecraft characteristics will be fixed:

- **Pointing**: the objective of the mission is to point to the Sun. Therefore, the reference direction, which will be used to define the desired orientation matrix, will be defined by a Sun pointing unit vector. Together with this direction, a second one must be defined. In this case this direction will be the one pointing from the cubesat to Earth. The reason is that having this orientation will potentially make easier the communications of the cubesat with the ground stations on Earth. The desired attitude matrix will be then defined as:

$$A^d_{BN} = \begin{bmatrix} \underline{x}_1 = \hat{\underline{S}}_B \\ \underline{x}_2 = \underline{x}_3 \times \underline{x}_1 \\ \underline{x}_3 = \hat{\underline{S}}_B \times \hat{\underline{r}}_{sc} \end{bmatrix}$$

- **Orbit**: as the only constraint is the altitude, a 500km altitude circular orbit will be considered. The other orbit parameters will be chosen in order to facilitate the case of study and avoid sources of errors and inaccuracies. Because the attitude determination with the sensors will be based on the knowledge of $\underline{r}$ and $\underline{b}$, a polar orbit, where those vectors are almost parallel, will induce an error on the estimation matrix, so an equatorial orbit will be chosen instead. As for the semi-major axis, having a constant altitude will render many variables to constants and simplify many computations (e.g air drag), so a circular 500km orbit will be chosen.

$$[a, e, i, \Omega, \omega, \theta_0] = [6871km, 0, 0°, 0°, 0°, 0°]$$

- **Initial condition**: the cubesat will be given an initial random angular velocity of 10°/s simulating a tumbling satellite. In addition, other initial quantities (such as the initial DCM) will be randomly initiated or tuned, depending on their origin.

- **Spacecraft**: 16 units cubesat. Usually each unit is about 10x10x10 cm and 1kg. It is worth to note that cubesats of 16U dimensions are not really common. In order to be more realistic dimension-wise, the MARIO spacecraft[2] has been taken as reference, so a cubesat of 25x25x50 cm will be considered, together with 2 solar panels of 20x44 cm when deployed. For the moment of inertia, due to lack of precise information, as a practical approximation the 12U LUMIO spacecraft[3] has been considered and linearly adapted to a 16U cubesat to yield a inertia matrix as follows:

$$J = \begin{bmatrix} 134.53 & 0 & 0 \\ 0 & 33.47 & 0 \\ 0 & 0 & 122.13 \end{bmatrix} 10^{-2}[kgm^2]$$

  The approximate total mass would be about 32 kg.

- **Actuators**: the spacecraft will be equipped with 3 magnetic torquers and 1 reaction wheel. Given the big dimensions of the spacecraft for a cubesat and the low number of actuators available, in order to have a better control over the spacecraft the selected actuators should have great capabilities. This will be further specified in subsection 3.4.

- **Sensors**: the spacecraft will be equipped with an earth horizon sensor, a magnetosensor and a gyroscope, further specified in subsection 3.5.

2 ADCS architecture (1 page)

The architecture of the attitude system will be as depicted in Fig. 1. In addition, Section 2 shows some critical aspects of the components.

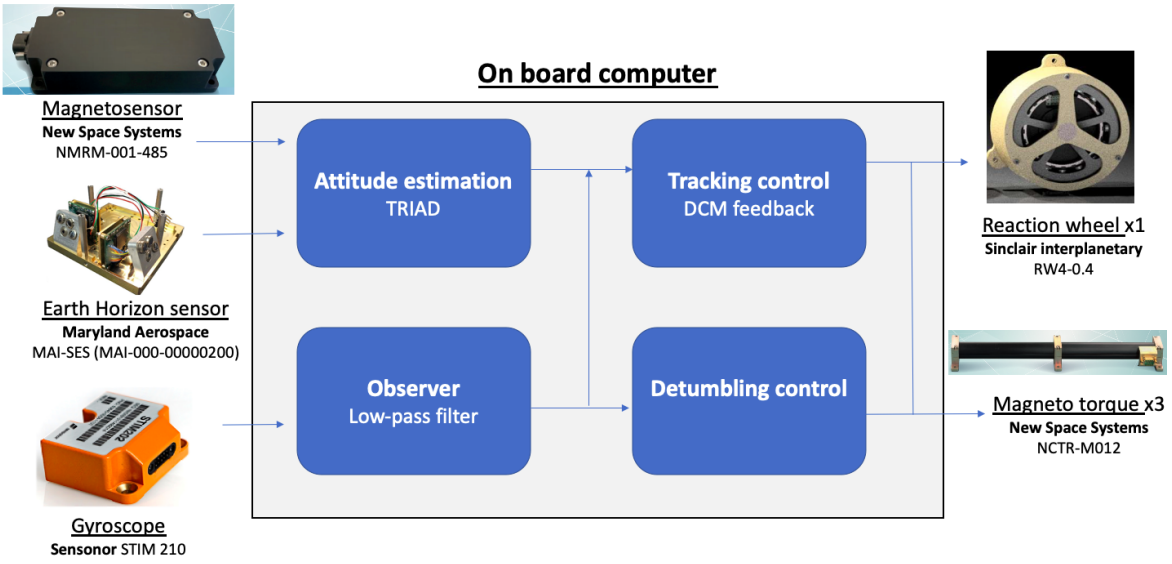

Figure 1: Sensors, actuators and interaction defining the attitude system architecture.

Component	Mass [g]	Dimensions [mm]
Reaction Wheels RW4-0.4	600	100x100x48
Magnetorquer NCTR-M012	120	94x15x13
Gyroscope STIM 210	52	38.6x44.8x21.5
EH sensor MAI-SES	33	43.2x31.8x20.7
Magnetosensor NMRM-001-485	67	96x45x20
TOTAL	872	——

Table 1: Components of the attitude system.

3 Model description (3-4 pages)

3.1 Dynamics

The attitude dynamics are represented by the Euler equations:

$$J \cdot \dot{\underline{\omega}} = \underline{\omega} \times (J \cdot \underline{\omega}) + \underline{u} + \underline{M}$$

where J is the inertia matrix expressed in the body frame (i.e diagonal); $\underline{\omega}$ is the angular velocity of the cubesat, $\underline{u}$ is the applied control torque by the actuators and $\underline{M}$ is the external torque disturbances affecting the cubesat.

3.2 Kinematics

Because the sensors models introduce the Direct Cosine Matrix (DCM), it is of convenience to express the kinematics of the system in the same way, following:

$$\dot{A}_{BN} = -[\underline{w}]^{\wedge} \cdot A_{BN}$$

where

$$[\underline{w}]^{\wedge} = \begin{bmatrix} 0 & -\omega_3 & \omega_2 \\ \omega_3 & 0 & -\omega_1 \\ -\omega_2 & \omega_1 & 0 \end{bmatrix}$$

It is worth noting that, as *Simulink*'s integrator is not structure preserving, A_{BN} has to be orthonormalized at each integration step. This orthonormalization is carried out by using the following formula:

$$A_{k+1}(t) = \frac{3}{2} \cdot A_k(t) - \frac{1}{2} \cdot A_k(t) \cdot A_k^T(t) \cdot A_k(t)$$

This process can be done more than once to ensure a proper accuracy over large computations. In this case, this iteration will be done twice, as the accuracy is satisfactory after it.

3.3 Perturbations

There are a number of disturbance torques affecting the attitude motion of the orbiting cubesat. Each one of them will be further developed in the following subsections.

3.3.1 Solar Radiation Pressure

The source of this perturbation comes from the photons expelled by the Sun that impact the surface of the cubesat, exchanging momentum with it in the process. The average pressure due to this radiation is:

$$P = \frac{F_e}{c}$$

with $c = 3 \cdot 10^8$ $[m/s]$ being the speed of light and $F_e = 1358$ $[W/m^2]$ the power at 500 km per unit surface.
A simplified equation for a flat panel is:

$$\underline{F} = -PA(\hat{S}_B \cdot \underline{\hat{n}}_s) \left[(1 - \rho_s)\hat{S}_B + (2\rho_s(\hat{S}_B \cdot \underline{\hat{n}}_s) + \frac{2}{3}\rho_d)\underline{\hat{n}}_s \right]$$

being $\underline{\hat{S}}_B = A_{BN}\underline{\hat{S}}_N$ the unitary relative position vector of the Sun with respect to the spacecraft; and ρ_d, ρ_s are the optical properties of the cubesat. Computing this force for each surface and adding

them up yield the total radiating force applied to the cubesat.
However, we have to take into account that only those surfaces in line of sight with the Sun (and also only when the satellite is not in eclipse, of course) will receive this radiation. Mathematically, only the surfaces satisfying $\underline{\hat{S}}_B \cdot \underline{\hat{n}}_s > 0$ will be taken into account. Then, the torque is given as:

$$\underline{T}_{SRP} = \begin{cases} \sum_{i=1}^{n} \underline{r}_i \times \underline{F}_i & \underline{\hat{S}}_B \cdot \underline{\hat{n}}_s > 0 \\ 0 & \underline{\hat{S}}_B \cdot \underline{\hat{n}}_s < 0 \end{cases}$$

where $\underline{r}_i$ is the position of the surface's centre of pressure with respect to the centre of mass.
It is worth to point out that not only the direct radiation coming from the Sun, but also the radiation reflected by the Earth is in some cases worth to include. It will be considered, again, only in the surfaces in line of sight with the Earth, and in a similar way than the previous one, but with a force of $F_e^E = 600\ [W/m^2]$.

3.3.2 Gravity gradient

The gravity gradient is a result of a non-uniform gravity field over the cubesat and therefore a torque acts on the satellite, as it can be seen in Fig. 2. Clearly, this perturbation is more significant in larger

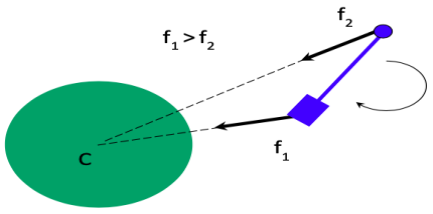

Figure 2: Gravity gradient torque diagram [1].

satellites. However, even if the resulting torque is small, when propagated over large times it can sum up to a significant resultant torque. The generated torque can be evaluated by an elementary force f acting on an elementary mass dm:

$$dM = -\underline{r} \times \frac{G m_t dm}{|R + r|^3} (\underline{R} + \underline{r}) dm$$

From which it can be derived (see [1]) that:

$$M = \frac{3\mu_E}{R^3} \cdot \begin{bmatrix} (I_z - I_y) c_2 c_3 \\ (I_x - I_z) c_1 c_3 \\ (I_y - I_x) c_1 c_2 \end{bmatrix}$$

with

$$\underline{c} = \begin{bmatrix} c_1 \\ c_2 \\ c_3 \end{bmatrix} = A_{BL} \begin{bmatrix} 1 \\ 0 \\ 0 \end{bmatrix}$$

3.3.3 Residual Magnetic Torque

It is caused by the interaction of the Earth's magnetic field with the local magnetic fields of the cubesat (mainly generated by the flow of a current in the electronics). The induced torque is described by:

$$\underline{M} = \underline{m} \times \underline{b}_B$$

where $\underline{m}$ is the residual magnetic induction due to currents in the satellite. It is difficult to model in a simulation, thus an average constant value of $\underline{m} = [0.1, 0.1, 0.1]^T [Am^2]$ will be used, as it represents an extreme case and ensures that the system is tested against a bad scenario.

On the other hand, $\underline{b}_B$ is the Earth's magnetic field as measured in the body frame. It can be derived from the inertial magnetic field vector as $\underline{b}_B = A_{BN}\underline{b}_N$. In order to obtain $\underline{b}_N$ Earth's magnetic field will be modelled using the magnetic dipole aproximation (see [1]) which yields:

$$\underline{b}_N = \frac{R^3 H_0}{r^3}[3(\underline{\hat{m}} \cdot \underline{\hat{r}})\underline{\hat{r}} - \underline{\hat{m}}]$$

where $\underline{r}$ is the position vector at the point where $\underline{b}_N$ is evaluated, R is the equatorial radius, $\underline{\hat{m}}$ is the unit vector along the dipole axis and $H_0 = \left((g_1^0)^2 + (g_1^1)^2 + (h_1^1)^2\right)^{1/2}$, where the Gaussian coefficients g and h are evaluated from experimental data.

3.3.4 Air drag

The interaction between the atmosphere and the cubesat can still be important in space, generating aerodynamic forces that derive into a torque. Aerodynamic torques represent the major disturbance for satellites lower than 400 km, and are considered negligible only above 700 km of altitude. As our orbit is at 500 km, this effect has to be taken into account. It can be modelled as follows:

$$\underline{M} = \sum \underline{r_i} \times \underline{F_i}$$

with

$$\underline{F_i} = -\frac{1}{2} C_d \rho(h,t) A_i v_r^2 \frac{\underline{v_r}}{\|\underline{v_r}\|}(\underline{\hat{n}_{si}} \cdot \frac{\underline{v_r}}{\|\underline{v_r}\|})$$

where C_d is the drag coefficient (typically 2.2); ρ is the air density at a certain height (in this case a constant $\rho = 4.39e^{-13}[kg/m^3]$); A_i is the area of surface i; $\underline{v_r}$ is the relative velocity between atmosphere and cubesat; $\underline{\hat{n}}$ is the unitary vector normal to the surface A_i and $\underline{r_i}$ is the position vector from the center of mass of the cubesat to the center of pressure of the surface A_i.

It is important to highlight that each surface is evaluated for $\underline{\hat{n}_{si}} \cdot \frac{\underline{v_r}}{\|\underline{v_r}\|} > 0$, otherwise $F_i = 0$. Lastly, in order to model the torque in the body frame, also the variables have to be evaluated in this same frame. So for example the relative velocity is computed as $\underline{v_r} = \underline{v_o} + \underline{\omega_E} \times \underline{R}$, being $\underline{v_o}$ the cubesat's velocity in the inertial frame, $\underline{R}$ its position and $\underline{\omega_E}$ the angular velocity of the Earth.

Fig. 3 depicts the sum of all the perturbations affecting the cubesat just explained above. As it can be noticed, the order of magnitude of the total perturbation is of the order of 10^{-6}, which means that it supposes a pretty small disturbance torque. However, this effect is more noticeable as time passes, and the overall effect during several orbits must be taken into account.

This torque is mainly caused by the air drag, due to the relatively low orbit design, and the magnetic force and the residual magnetic field due to the electronics on board (remember that a conservative value of $\underline{m} = [0.1; 0.1; 0.1]$ $[Am^2]$ was taken, so hopefully it will be lower during a real mission).

3.4 Actuators

3.4.1 Reaction wheel (RW) Sinclair interplanetary RW4-0.4 [9]

A reaction wheel is an actuator based on acceleration of spinning rotors. It can only exchange angular momentum but not produce a net torque. Only one reaction wheel is allowed in the cubesat, which

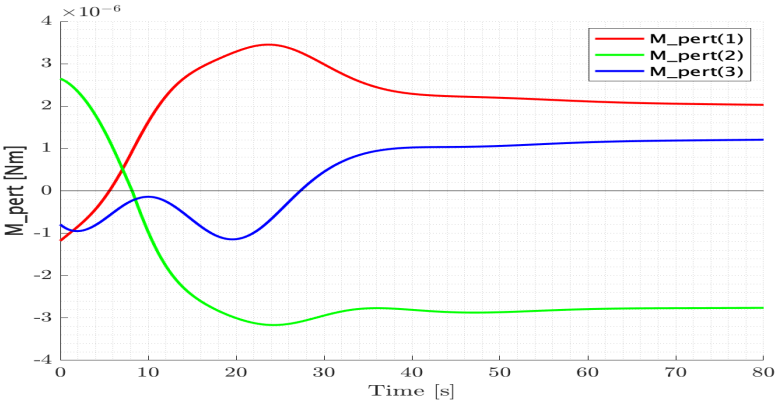

Figure 3: Sum of momentum of all perturbations (SRP, gravity gradient, RMT and air drag).

is a major drawback as the usual number of reaction wheels to successfully control the attitude is four. Therefore, in order to take the most of our only reaction wheel, a really capable one has been chosen, *Sinclair RW4-0.4 3*, of maximum momentum storage $h_{r_{max}} = 400[mNms]$ and maximum torque $\dot{h}_{r_{max}} = 100[mNm]$ [9]. The high momentum storage will prolong the reaction wheel work before saturation.

The chosen configuration for the RW has been the following:

$$A = \begin{bmatrix} 1/\sqrt{(3)} \\ 1/\sqrt{(3)} \\ 1/\sqrt{(3)} \end{bmatrix}$$

which means that it is oriented equally in the three body axes. Having just one reaction wheel is a disadvantage, as the most common configurations for satellites using reaction wheels require of usually four actuators(despite three being enough for an effective control, a fourth one is usually added for redundancy). This way three can be directed along the principal axis and another one diagonally, or they can also be arranged in a pyramid configuration.
Different orientations for the reaction wheel have been tested, but an equilibrated configuration was the most consistent one. For a known initial de-tumbling, favouring one direction over others can be useful, but since we cannot predict the initial direction of the de-tumbling velocity, this is the most reliable configuration so that the reaction wheel is always kept far from saturation. It also yields the faster de-tumbling results.

The equation that govern the RW dynamics is:

$$\dot{\underline{h}}_r = -A^* \cdot (\underline{u}_i + \underline{\omega} \times (A \cdot \underline{h}_r))$$

where A^* is the pseudo inverse matrix of A, $\dot{\underline{h}}_r$ is the torque $[Nm]$ and $\underline{h}_r$ is the angular momentum $[Nms]$ of the reaction wheel around its spin axis.

For the control torque:

$$\underline{u}_r = -A \cdot \dot{\underline{h}}_r - \underline{\omega} \times (A \cdot \underline{h}_r)$$

3.4.2 Magneto torque (MT) New Space Systems NCTR-M012 [5]

Magnetic actuators generate torque by inducing a magnetic dipole in a coil, surrounded by the EArth's magnetic field. They are essentially rods with a ferromagnetic core with winding coils around the core

which supply current, interacting with the Earth's magnetic field. As a result of this interaction, a torque is generated.
The maximum value of the magnetic dipole selected is of 1.19 $[Am^2]$, which is pretty high for a cubesat (typical value for a 3U cubesat is 0.4 Am^2). As said before, given that this is a 16U cubesat and the fact that only one reaction wheel is available, the magnetic torquer will be just powerful enough so that a decent (in terms of time) de-tumbling can be achieved. Also, it is important to have reliable magneto torques due to their many advantages (lightweight, energy efficient, no fuel).
The magnetic torque generated obeys:

$$\underline{M} = \underline{m} \times \underline{b}$$

with $\underline{b}$ is the Earth's magnetic field (see subsection 3.3.3).
Usually there are 3 rods for 3-axis control. However, it is an underactuated system, since when a rod is aligned with the magnetic field it will not produce torque. Luckily, during de-tumbling, the cubesat is rotating rapidly so the direction of the magnetic field changes constantly.

3.5 Sensors

3.5.1 Magnetosensor (MS) NMRM-001-485 [6]

Using three pairs of nuclei the components of the magnetic field can be measured. They are usually placed as far as possible from the electronics to minimize interference and noise from on-board electronics, still, other effects such as solar wind and uncertainties in the modelling introduce large inaccuracies in the model.

The dipole Earth's magnetic field approximation (see subsection 3.3.3) will be used. The angular error will be:

$$\underline{b}_B^{ideal} = A_\epsilon A_{BN} \underline{b}_N$$

where A_ϵ is the error matrix that represents an angular misalignment $d\theta$ with respect to a prescribed direction:

$$A_\epsilon = \begin{bmatrix} \cos\psi\cos\theta & \cos\psi\sin\theta\sin\phi + \sin\psi\cos\phi & -\cos\psi\sin\theta\cos\phi + \sin\psi\sin\phi \\ -\sin\psi\cos\theta & -\sin\psi\sin\theta\sin\phi + \cos\psi\cos\phi & \sin\psi\sin\theta\cos\phi + \cos\psi\sin\phi \\ \sin\theta & -\cos\theta\sin\phi & \cos\theta\cos\phi \end{bmatrix}$$

In a magnetosensor the error depends on the altitude of the orbit. They have an accuracy of 5° at 200km to 1° at 5000km. In this case (h=500km) the value will be $d\theta = 2°$ (non-linear dependance). From the datasheet of the sensor [6] the sensor's noise is characterized at 8 nT at 1 Hz, from which it can be modelled as a white noise $\underline{n}$. Therefore, the modelled magnetosensor will be:

$$\underline{b}_B^{MS} = A_\epsilon A_{BN} \underline{b}_N + \underline{n}$$

3.5.2 Earth Horizon Sensor (EH) Maryland Aerospace MAI-000-00000200 [7]

It is basically a series of thermopile detectors that detect incident power from electromagnetic radiation via the heating of a material with a thermal sensitive resistance. The Earth Horizon Sensor measures the position vector of the cubesat with respect to the Earth in the body frame $\underline{r}_B$. Similarly to the previous sensor, it has been modelled as:

$$\underline{r}_B^{EH} = A_\epsilon A_{BN} \underline{r}_N$$

In this case, the sensor's accuracy is 0.25°.

3.5.3 Gyroscope STIM 210 [8]

Gyroscopes measure angular velocities. The classical ones have a spinning rotor and a mechanical sensor, but there are others based on lasers. They are characterized by a moment of inertia I_R and an angular velocity ω_R known. The torque measurements $\underline{M}$ can be related to the angular velocity of the cubesat by:

$$\underline{\omega} = \frac{\underline{M}}{I_R \cdot \omega_R}$$

Furthermore, we will model a real gyroscope with real errors, mainly two different bias errors provided by manufacturers:

- ARW: the angular random walk, attributed to thermo mechanical noise of the system $\underline{n} = \sigma_n \underline{\xi}_n$, modelled as white Gaussian noise with zero mean and $\sigma_n = 0.15 deg/\sqrt{h}$ standard deviation.
- RRW: rate random walk, attributed to electronic noise $\dot{\underline{b}} = \sigma_b \underline{\xi}_b$, modelled as white Gaussian noise with zero mean and standard deviation $\sigma_b = 0.30 deg/h$ at 262 Hz

so the angular velocity measured by the sensor is:

$$\underline{\omega}^{gyro} = \underline{\omega}^{real} + \underline{n} + \underline{b}$$

Fortunately, the noise can be filtered, improving the performance of the gyro. An observer as follows has been implemented:

$$J\underline{\omega}^{est} = J \cdot \underline{\omega}^{est} \times \underline{\omega}^{est} + \underline{u_r} - \alpha(\underline{\omega}^{est} - \underline{\omega}^{sens})$$

where α is a tuning parameter. Looking for the best accuracy-speed trade-off, the optimal value has been found to be $\alpha = 0.05$.

4 Control and determination algorithms (2 pages)

The mathematical analysis of attitude determination is complicated by the fact that attitude determination is necessarily underdetermined or overdetermined (one measurement is not enough, two measurements are too many), so all attitude determination algorithms are really attitude estimation algorithms. It is needed a combination of sensors and models to gather vectors in body and inertial frames, which are then used on different algorithms to determine the attitude. It takes at least two vectors to estimate the attitude, so two sensors are needed (e.g Earth horizon and magnetosensor). By relating the body and inertial vectors through a rotation matrix, the attitude can be known, so determining the attitude of a spacecraft is equivalent to determining the rotation matrix [4].

4.1 Attitude determination algorithm (TRIAD)

In this case it will be based on the measurements from the Earth horizon sensor $\underline{r}_B$ and the magnetosensor $\underline{b}_B$; and the mathematical models that yield us the inertial measurements $\underline{r}_N$ and $\underline{b}_N$. There are several determination algorithms, namely the SVD, TRIAD, QUEST and q-method (detailed in [4]).

For this study, the TRIAD algorithm has been chosen. It is the simplest algorithm, so the other methods involving more complex calculations also require more computational time. In addition, being available only two measurements, the other methods yield results not that different to the TRIAD ones, so the lack of precision of TRIAD with respect to the others is diminished. Lastly, the QUEST

and q-method involve quaternions and Gibbs vector, which in turns requires a conversion to DCM (introducing errors, increasing computational time and adding discontinuities).

Call two measurements p and q, and a and b their directions in inertial frame. Associate p to the unit vector s_1 and the direction a to the unit vector v_1. Two orthogonal frames can be defined:

$$\underline{s}_1 = \underline{p}; \quad \underline{s}_2 = \frac{\underline{p} \times \underline{q}}{|\underline{p} \times \underline{q}|}; \quad \underline{s}_3 = \underline{p} \times \underline{s}_2$$

$$\underline{v}_1 = \underline{a}; \quad \underline{v}_2 = \frac{\underline{a} \times \underline{b}}{|\underline{a} \times \underline{b}|}; \quad \underline{v}_3 = \underline{a} \times \underline{v}_2$$

so that $\underline{s}_1, \underline{s}_2, \underline{s}_3$ and $\underline{v}_1, \underline{v}_2, \underline{v}_3$ are orthogonal. Then it can be written that $V^{-1} = V^T$ so that $A = SV^{-1} = SV^T$. Notice that to minimize errors, $\underline{p}$ should be measured with the maximum precision and $\underline{q}$ should be as orthogonal as possible to $\underline{p}$. Clearly, if $\underline{p} = \underline{q}$, the matrices would not be orthonormal and the attitude determination would not work.

4.2 Detumbling control algorithm

The de-tumbling will be carried out by the magneto torquers and the reaction wheel. The control algorithm implemented for the magneto torquers is:

$$\underline{m} = -k\dot{\underline{b}}$$

with a tuning parameter $k = 1 \cdot 10^6$. Once again, this control only ensures convergence in 2-axis as the third magnetic torquer may be aligned with the magnetic field, not producing torque, but due to the de-tumbling condition this will only happen for a very brief period of time. It is a very common and used feedback control on Cubesats due to its simplicity (it is only needed the time derivative of the sensor measurement) but it can also derivate inaccuracies for noisy signals. In this cases, the approximation $\dot{\underline{b}} \approx \underline{b} \times \underline{\omega}$ is a good alternative, needing only of a magnetometer and a gyro.
We can differentiate the equation

$$V = \frac{1}{2}\underline{\omega}^T J \underline{\omega}$$

to obtain $\dot{V}(\underline{\omega}) = \underline{\omega}^T \underline{u}$. Then, a $\underline{u}$ must be chosen so that $\underline{\omega}^T \underline{u} < 0$. The implemented control algorithm for the reaction wheel is as follows:

$$\underline{u} = -k\underline{\omega}$$

with a tuning parameter $k = 1$. Implementing this algorithm to the dynamics of the reaction wheel (presented in subsection 3.4.1) ensures global asymptotic stability. It has been chosen over other stable controls options due to its continuous behaviour, better suited for a reaction wheel rather than an "on-off" controller type, more suited to thrusters.

4.3 Tracking control algorithm

It will be based on DCM, being this one faster than other alternatives such as a quaternion feedback. Being the Lyapunov function:

$$V = \frac{1}{2}(\underline{\omega} - \underline{\omega}^{ref})^T \cdot (\underline{\omega} - \underline{\omega}^{ref}) + k_2 \cdot tr(I - A^{err})$$

To ensure asymptotic stability $\dot{V}$ must be satisfied when $A^{err} \neq I$ and $\underline{\omega} \neq \underline{\omega}^{ref}$, so the implemented control law is:

$$\underline{u}^{id}(t) = \underline{\omega}(t) \times J \cdot \underline{\omega}(t) - k_1 \cdot J \cdot (\underline{\omega}(t) - \underline{\omega}^{ref}(t)) - k_2 \cdot J \cdot (A_e^T - A_e)^V$$

being $A_e = A_{BN}^{est}[A_{BN}^{d}]^T$ and $k_1 = 0.05$, $k_2 = 0.5 * k_1^2$.
It is important to take into account that the sensors cannot work for angular velocities $|\underline{\omega}| > 0.5$ $[deg/s]$. Even though after the detumbling the cubesat will be left with a lower angular velocity, the tracking control can require large rotations, exceeding this treshold. If this is the case, the attitude determination could not work, so the controller would not be able to estimate A^{err}, making impossible for the control law to be computed.
This problem can be avoided by defining a more complex control law that triggers whenever the angular velocity approaches the sensor's threshold and the control law orders to increase it. It would look like:

$$\underline{u}^{\pm}(t) = \underline{\omega}(t) \times J\underline{\omega}(t) - k_1 J \left(\underline{\omega}(t) \mp 0.45 \frac{\pi}{180} \cdot \begin{bmatrix} \sqrt{(3)}/3 \\ \sqrt{(3)}/3 \\ \sqrt{(3)}/3 \end{bmatrix} \right)$$

The complete control law looks like:

$$\underline{u}_i^{track}(t) = \begin{cases} \underline{u}_i^{+}(t) & \text{if} \quad \omega_i(t) \geq 0.4 \cdot \frac{\pi}{180} \quad \text{and} \quad u_i^{id}(t) > 0 \\ \underline{u}_i^{-}(t) & \text{if} \quad \omega_i(t) \leq -0.4 \cdot \frac{\pi}{180} \quad \text{and} \quad u_i^{id}(t) < 0 \\ \underline{u}_i^{id}(t) & \text{else} \end{cases}$$

5 Results (12-13 pages)

5.1 Detumbling phase

To make sure the simulation ends when an acceptable angular velocity is reached, a *"while loop"* has been implemented so that it prolongs the simulation time until $||\underline{\omega}|| < ||\underline{\omega}_{req}||$, being in this case $||\underline{\omega}_{req}|| = 0.5$ $[deg/s] \cdot 0.5$ [safety factor].
Fig. 4 shows the angular velocity during the detumbling, which rapidly decays to values under $\underline{\omega}_{req}$.

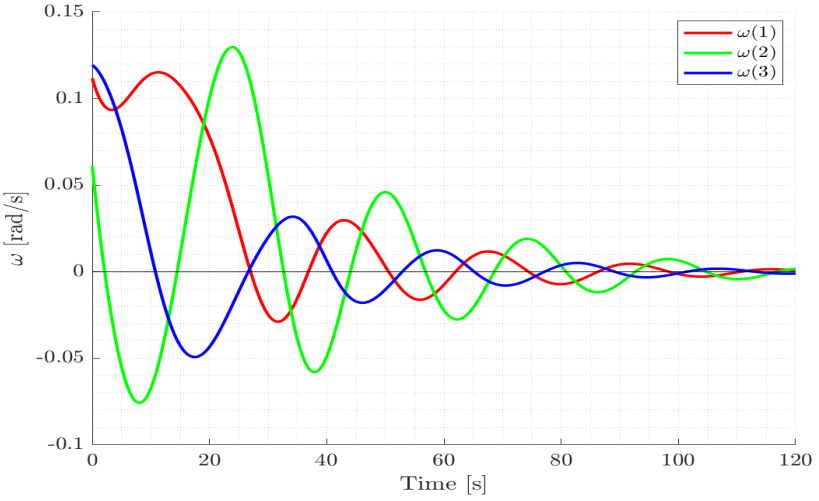

Figure 4: De-tumbling angular velocity.

As it can be seen from Fig. 5 the reaction wheel is far from its saturation limit ($0.4[Nms]$). On the other hand, Fig. 6 shows that the magnetometers are working at their full capabilities ($1.19\ [Am^2]$) during all the de-tumbling phase. Therefore, more powerful magneto torquers could reduce the stabilising time, but it would increase the mass of the actuators, and being the time already small, they are enough to help stabilise the cubesat.

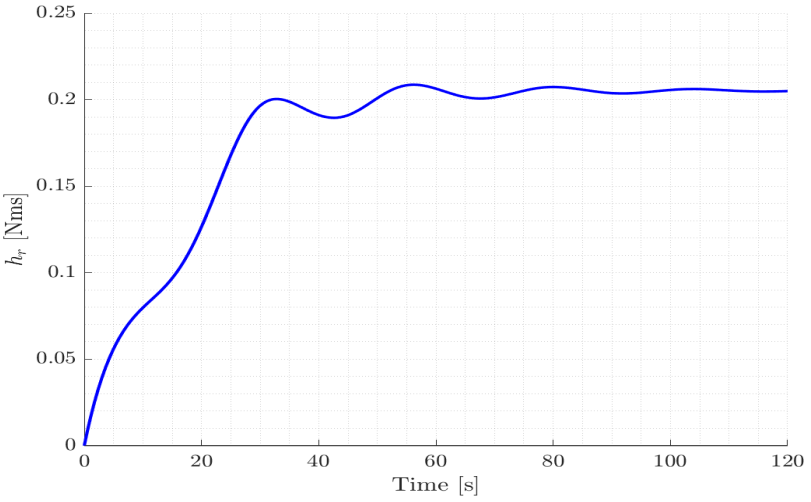

Figure 5: Reaction wheel momentum demand during de-tumbling.

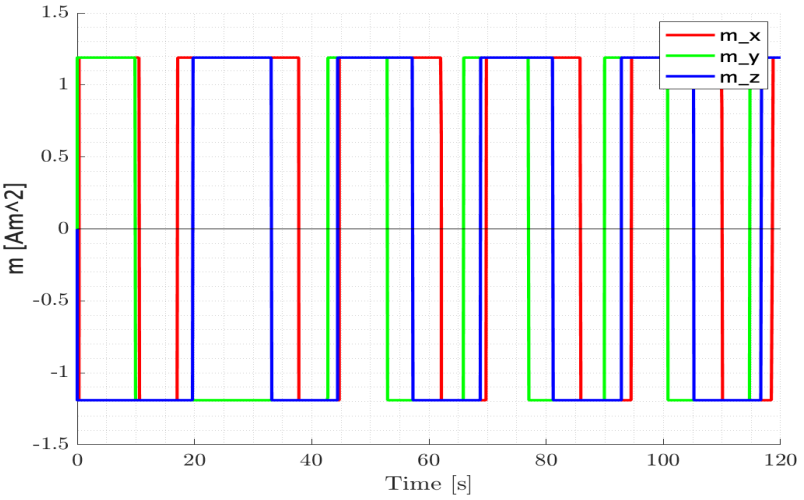

Figure 6: Magnetic torquer demand during de-tumbling.

Fig. 7 depicts the control torque applied to the cubesat in order to de-tumble it and how rapidly it diminishes as the cubesat decelerates. Lastly, Fig. 8 shows the error between the real angular velocity

and the one estimated by the gyro. It is worth to notice that the error is pretty low, of the order of 10^{-3} $[rad/s]$.

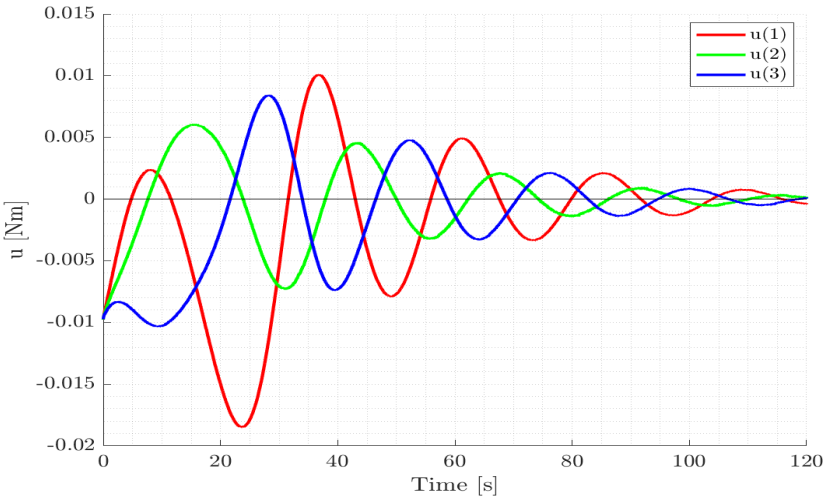

Figure 7: Control torque $\underline{u}$.

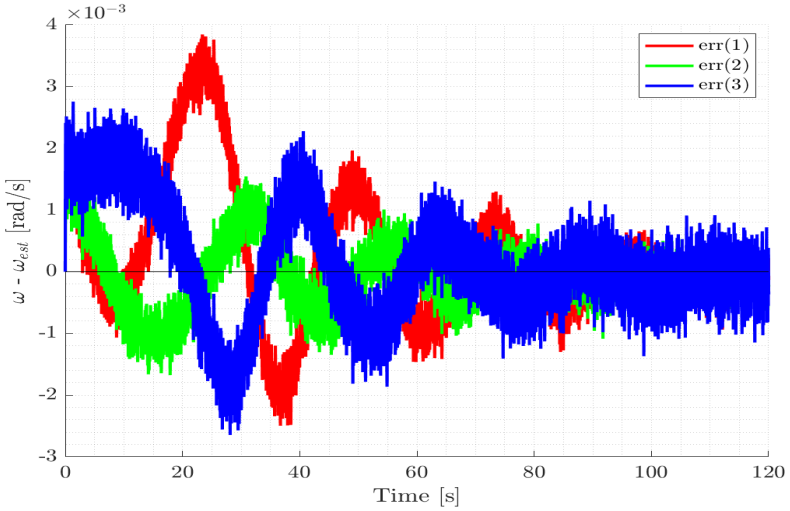

Figure 8: Error between the real angular velocity and the gyroscope estimated one during the detumbling phase.

5.2 Tracking phase

Fig. 9 shows the angular velocity of the cubesat during the tracking phase. It starts with the residual angular velocity left from the detumblilng, and it mantains while the cubesat is orienting itself in or-

der to point to the desired direction. Then, once perfectly oriented, this velocity keeps decaying to zero.

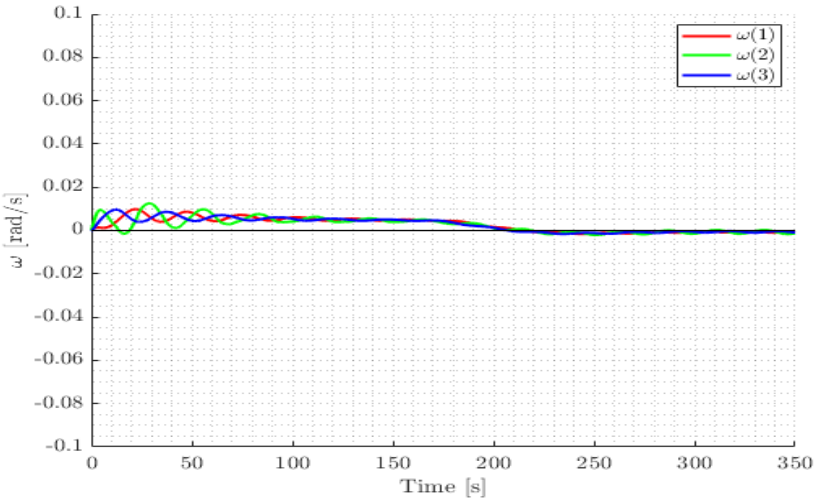

Figure 9: Angular velocity during the tracking phase$[rad/s]$.

This time the controller has been fed with the estimated angular velocity $\underline{\omega}_{est}$ from the gyroscope plus observer. As before, the error between the real angular velocity and the estimated one has been computed (see Fig. 10). Because the error between them is so low, both in the de-tumbling and the tracking phase, whenever a longer simulation is needed it is much more convenient to omit the model with the gyroscope, as it does not add much more accuracy but it is much more computationally demanding.

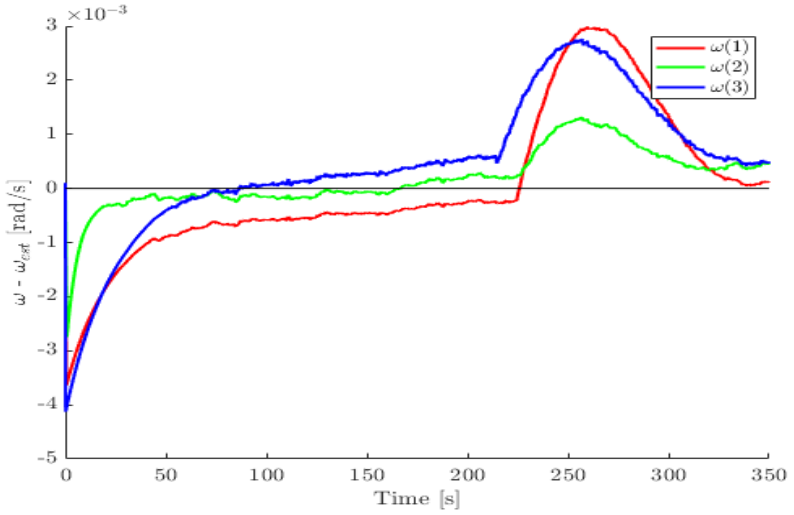

Figure 10: Angular velocity error between the actual and the estimated angular velocity during the tracking phase[rad/s].

Fig. 11 shows the pointing error, this is the difference (in [deg]) between the cubesat pointing and the desired direction pointing. It starts with a random pointing consequence of the detumbling phase, and by comparing the desired attitude matrix A^d_{BN} with the actual one A_{BN} the attitude system corrects the orientation of the cubesat until it approximates to 0°.

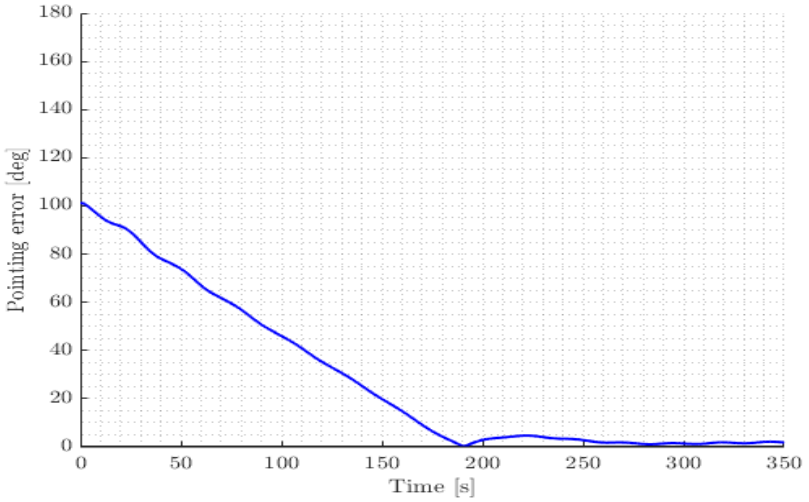

Figure 11: Pointing error during tracking phase [deg].

Fig. 12 shows the momentum exerted by the reaction wheel in order to adjust the cubesat's attitude. Once again, the reaction wheel has been properly sized so it is far from saturation.

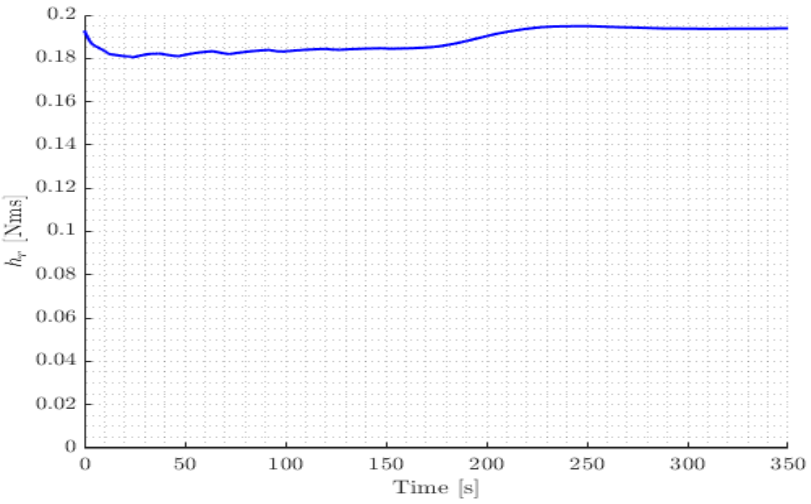

Figure 12: Reaction wheel momentum during tracking phase $[Nms]$.

Lastly, Fig. 13 depicts the differences between the ideal control computed by the system in order to point towards the desired direction and the actual control that is exerted by the reaction wheel, which closely follows the ideal one.

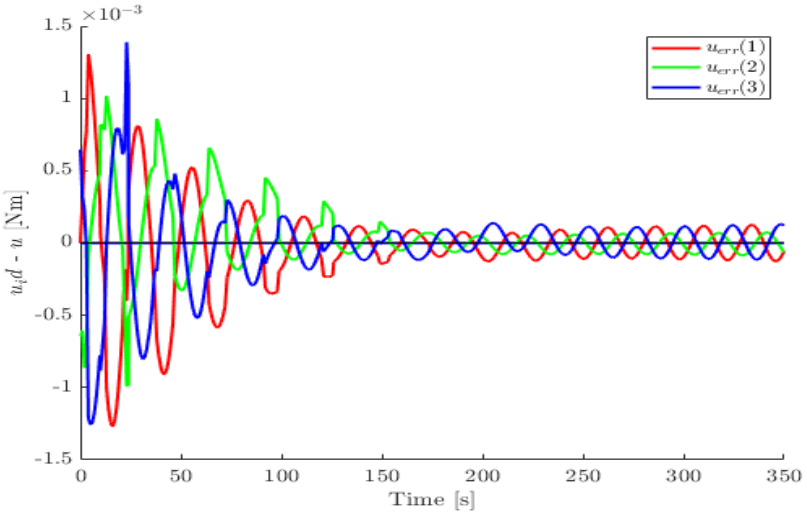

Figure 13: Error between ideal feedback control and real control applied by the reaction wheel$[Nm]$.

6 Conclusion (max 1 page)

- The designed attitude control system is reliable. Different random initial conditions (concerning angular velocity and attitude matrix) have been tested, resulting in successful results, only

depending on convergence times.

- The pointing error, the difference between the actual attitude and the desired one, is influenced primarily by the estimation error (actual attitude vs. estimated one by the sensors).
- There may exist more complex and better control laws, able to reduce the command error. However, in this case they will not influence greatly the results, as the major source of errors is the estimation error. Therefore, until reducing it to the same level as the command error, developing and implementing better control laws will have negligible effects.
- As mentioned in the *Attitude determination algorithm* section, the TRIAD algorithm is the best suited for the project. There are only two independent measures to estimate the attitude of the cubesat, other determination algorithms are not much more accurate but they are more computationally expensive.
- In addition to the last conclusion point, including additional sensors to the cubesat would be a good idea whenever the pointing error accuracy wants to be increased. In this case, the TRIAD algorithm most surely would not be the best choice. The SVD algorithm would be then the most suited, as it employs the DCM.
- The model, in absence of the gyroscope, allows for longer simulations without inducing relevant errors compared to the model with gyroscope. This is because the gyroscope system induces a smaller integration stepsize, making it more computationally expensive.
- Another different approach to reduce computation time in the tracking phase of the mission is linearise the model around the reference condition:

$$\delta\underline{\omega} = \underline{\omega} - \underline{\omega}^{ref}$$
$$\delta A_{err} = A_{BN}^{est}[A_{BN}^{d}]^T - I$$

  δA_{err} and A_{err} are equivalent because only components out of the diagonal are employed.
- The tuning parameters, such as the control law onesk_1, k_2 and the gyro observer α are the key to the error made and the simulating time of the model. A good trade-off between error and computation time must be reached.
- In case the gyroscope is greatly affected by noise, or it cannot be filtered properly, it can be substituted by a Kalman filter. In turn, it will be more computationally costly but it will also render higher accuracy.
- As mentioned in the *Detumbling phase* section, the de-tumbling is mainly done by the reaction wheel. However, the magneto torquers, which work to full capabilities for almost all the de-tumbling time, manage to reduce the de-tumbling time when compared with a "solo" reaction wheel de-tumble time.
- It is worth to notice that there are some disturbances that arise in real missions that have not been taken into account, such as control misalignment (jitter), flexible parts and sloshing.
- Despite having taken care into account the space environment perturbations (SRP, air drag, gravity gradient, magnetic field torque) more precise models can be implemented in order to better model the perturbations the cubesat will suffer.

List of Figures

List of Tables

References

[1] Biggs,J.D. *Spacecraft Attitude and Control lecture notes*. Politecnico di Milano, 2019.

[2] Mani, Karthik V. & Casado, Alvaro & Franzese, Vittorio and Topputo, Francesco & Cervone, Angelo. *Systems Design of MARIO: Stand-alone 16U CubeSat from Earth to Mars*. October 2019.

[3] Romero-Calvo, Alvaro & Biggs, James & Topputo, Francesco. *Attitude Control for the LUMIO CubeSat in Deep Space.*. 2019.

[4] Chris Hall. *Chapter 4. Attitude determination.*. March 18, 2003

[5] New Space System *NCTR-M012 datasheet*.

[6] New Space System *NHRM-001-485 datasheet*.

[7] Maryland Aerospace *MAI-000-00000200 datasheet*.

[8] Sensonor *STIM210 datasheet*.

[9] Sinclair interplanetary *RW4-0.4 3 datasheet*.